

Importance of π -Stacking Interactions in the Hydrogen Atom Transfer Reactions from Activated Phenols to Short-Lived *N*-Oxyl Radicals

Marco Mazzonna,[†] Massimo Bietti,[‡] Gino A. DiLabio,^{*,§,||} Osvaldo Lanzalunga,^{*,†} and Michela Salamone[‡]

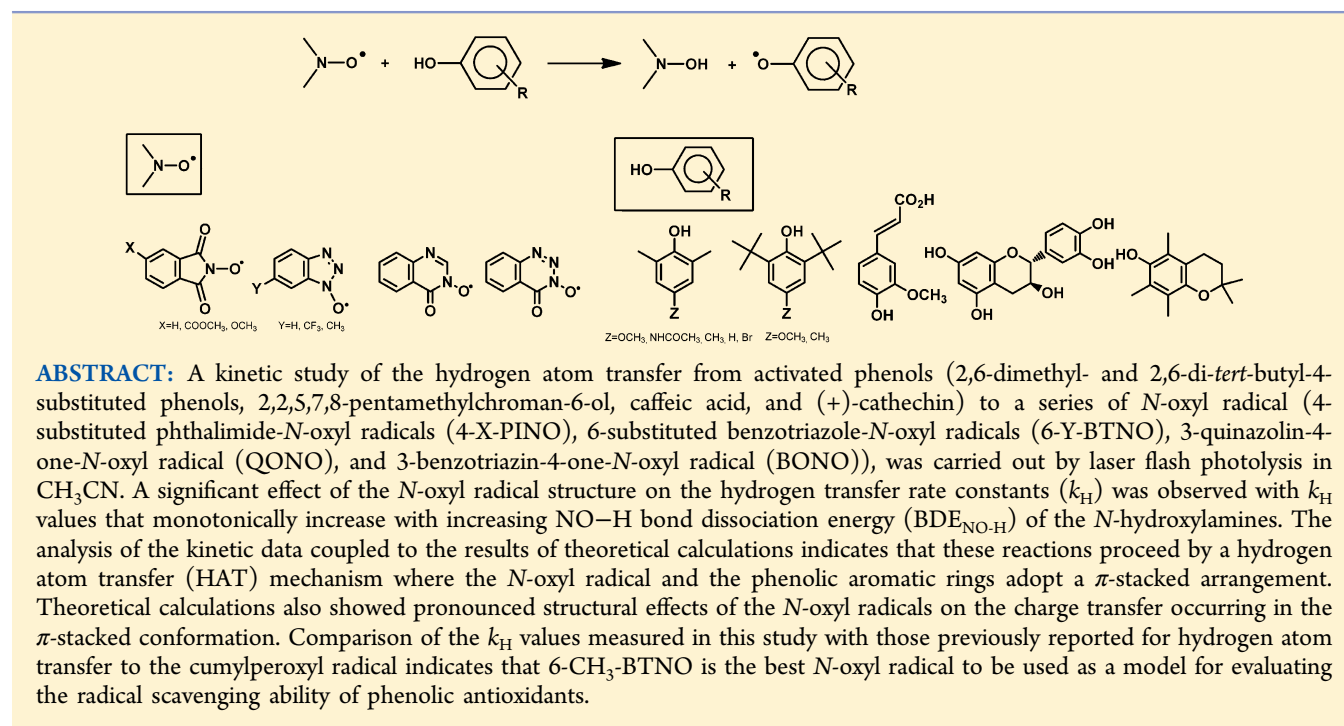
[†]Dipartimento di Chimica and Istituto CNR di Metodologie Chimiche (IMC–CNR), Sezione Meccanismi di Reazione, c/o Dipartimento di Chimica, Sapienza Università di Roma, P.le A. Moro, 5, I-00185 Rome, Italy

[‡]Dipartimento di Scienze e Tecnologie Chimiche, Università “Tor Vergata”, Via della Ricerca Scientifica, 1, I-00133 Rome, Italy

[§]National Institute for Nanotechnology, National Research Council of Canada, 11421 Saskatchewan Drive, Edmonton, Alberta, Canada T6G 2M9

^{||}Department of Chemistry, University of British Columbia, Okanagan, 3333 University Way, Kelowna, British Columbia, Canada V1V 1V7

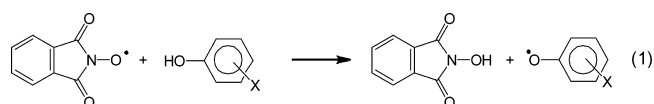
Supporting Information



INTRODUCTION

In recent years the reactivity of short-lived *N*-oxyl radicals such as the phthalimide-*N*-oxyl radical (PINO) and the benzotriazole-*N*-oxyl radical (BTNO) in hydrogen atom transfer from C–H and O–H bonds has been the object of extensive investigation.^{1–6} The interest in the reactions promoted by *N*-oxyl radicals is associated with the key role played by these reactive species in both metal-catalyzed and transition-metal-free aerobic oxidation of several classes of organic compounds^{1,7} and in the oxidative degradations promoted by the laccase/*N*-hydroxylamine/O₂ system.⁸ The latter process has found application in the degradation of lignin⁹ and of organic pollutants,¹⁰ decolorization of dyes,¹¹ and in synthetically useful procedures.¹²

Hydrogen atom transfer from phenolic O–H bonds to PINO (eq 1) has been analyzed in detail.^{13,14} This reaction is

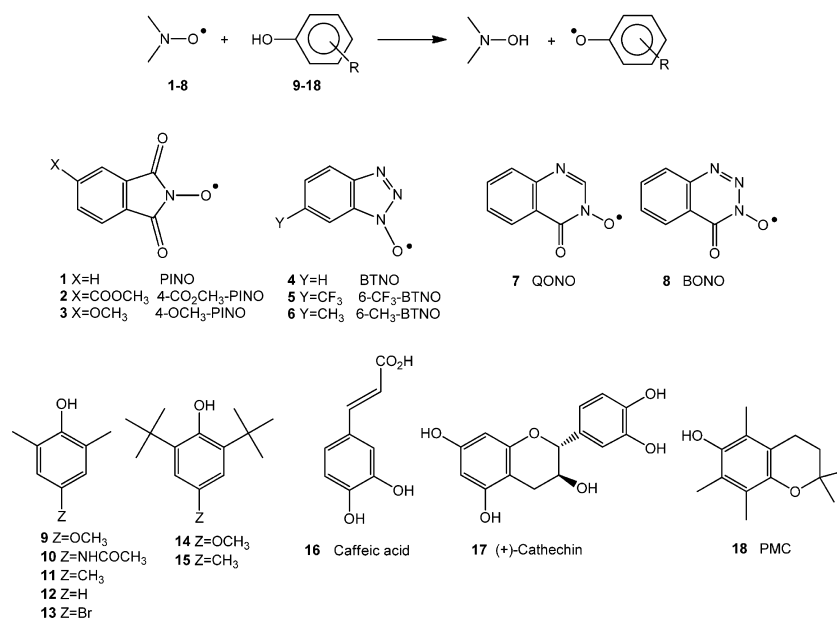


particularly interesting since it can occur as part of the oxidative degradation of the abundant phenolic residues of lignin promoted by the laccase/O₂ system mediated by *N*-hydroxyphthalimide (NHPI).^{8j} In addition, it has been proposed that the

Received: April 8, 2014

Published: May 1, 2014

Scheme 1



analysis of the PINO reactivity with phenols may represent a tool for evaluating the radical scavenging ability of phenolic antioxidants.^{13,14} This assessment was based on the similar bond dissociation energies (BDE) of the NO–H bond of NHPI formed after hydrogen transfer to PINO (88 kcal/mol)^{4,6} and that of the OO–H bonds formed by alkylperoxy radicals (89 kcal/mol for *t*BuOO–H).¹⁵ However, it was noted that caution should be taken when comparing the reactivity of these two classes of oxygen-centered radicals. Accordingly, a significantly higher reactivity of PINO with respect to alkylperoxy radicals was observed in hydrogen abstraction from phenolic O–H bonds,^{14,16} rationalized on the basis of a greater contribution of polar effects in the reactions promoted by PINO.^{1,3} Moreover kinetic studies and theoretical calculations for the reaction of PINO with activated phenols indicated that this process occurs by a hydrogen atom transfer (HAT) mechanism with a contribution from charge transfer (CT) deriving from the π -stacking of the phenolic and PINO aromatic rings.¹⁴ This mechanism is therefore somewhat different from the proton-coupled electron transfer (PCET) process suggested to be operative in the reaction of alkylperoxy radicals with phenolic antioxidants where the overlap of the inner oxygen peroxy lone-pair with the π -orbitals of the ring moiety of the phenol provides a channel for electron transfer.¹⁷

The work reported here reflects an interest in hydrogen atom transfer reactions between phenols and short-lived *N*-oxyl radicals and on the effects of noncovalent interactions in radical reactions. To investigate the effects of the structure of the *N*-oxyl radicals on the role played by CT interactions on the hydrogen transfer process, a time-resolved kinetic study in CH₃CN of the reactions of activated phenols including natural phenolic antioxidants (2,6-dimethyl- and 2,6-di-*tert*-butyl-4-substituted phenols (9–15), caffeic acid (16), (+)-catechin (17), and 2,2,5,7,8-pentamethylchroman-6-ol (PMC, 18)) with a series of *N*-oxyl radicals: 4-substituted phthalimide-*N*-oxyl radicals (4-*X*-PINO, 1–3),¹⁸ 6-substituted benzotriazole-*N*-oxyl radicals (6-*Y*-BTNO, 4–6), 3-quinazolin-4-one-*N*-oxyl radical (QONO, 7), and 3-benzotriazin-4-one-*N*-oxyl radical (BONO, 8) has been

carried out. The structures of activated phenols and *N*-oxyl radicals are shown in Scheme 1.

Theoretical calculations were performed in order to estimate the O–H bond dissociation energies (BDEs) of the *N*-hydroxylamines 1H–8H precursors of aminoxy radicals 1–8. Density-functional theory (DFT) with a continuum solvent model was used to compute rate constants of the reactions of aminoxy radicals with one of the most reactive phenols (4-methoxy-2,6-dimethylphenol (9)) in order to develop a deeper insight into the energetics and dynamics of the hydrogen transfer process.

RESULTS

Time-Resolved Studies. In the laser flash photolysis (LFP) experiments, *N*-oxyl radicals 1–8 were produced by hydrogen transfer from the corresponding *N*-hydroxy derivatives 1H–8H: 4-*X*-*N*-hydroxyphthalimides (4-*X*-NHPIs, 1H–3H), 6-*Y*-*N*-hydroxybenzotriazoles (6-*Y*-HBTs, 4H–6H), 3-hydroxyquinazolin-4-one (NHQO, 7H), and 3-hydroxybenzotriazin-4-one (NHBO, 8H) to the cumyloxy radical (eq 3 in Scheme 2).¹⁹ The latter species was generated by 355 nm LFP of an acetonitrile

Scheme 2

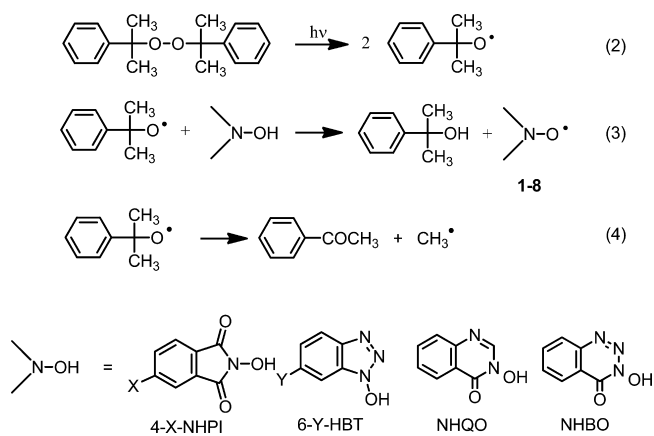
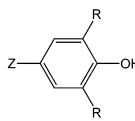
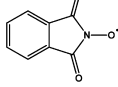
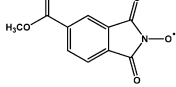
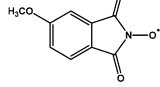


Table 1. Second-Order Rate Constants k_H ($M^{-1} s^{-1}$) for the Reactions of 4-Substituted Phthalimide-*N*-oxyl Radicals (4-*X*-PINO, 1–3) with Phenols 9–18 Measured at $T = 25$ °C

	BDE (kcal/mol)	k_H ($M^{-1} s^{-1}$) ^a		
		PINO (1) ^b  $\lambda_{max}=380$ nm	4-CO ₂ CH ₃ -PINO (2)  $\lambda_{max}=380$ nm	4-CH ₃ O-PINO (3)  $\lambda_{max}=490$ nm
9 R=CH ₃ , Z=OCH ₃	79.7 ^b	5.4×10^6	8.9×10^6	4.2×10^6
10 R=CH ₃ , Z=NHCOCH ₃	n.d.	2.4×10^6	6.2×10^6	2.1×10^6
11 R=CH ₃ , Z=CH ₃	82.7 ^c	2.9×10^5	4.3×10^5	1.9×10^5
12 R=CH ₃ , Z=H	84.5 ^c	3.2×10^4	4.2×10^4	2.2×10^4
13 R=CH ₃ , Z=Br	85.0 ^b	2.0×10^4	3.1×10^4	1.8×10^4
14 R= <i>t</i> Bu, Z=OCH ₃	78.3 ^c	1.6×10^5	2.0×10^5	1.3×10^5
15 R= <i>t</i> Bu, Z=CH ₃	81.0 ^c	1.3×10^4	1.9×10^4	1.2×10^4
16 Caffeic acid	81.9 ^{d,e}	8.2×10^4	1.3×10^5	7.4×10^4
17 (+)-Catechin	81.1 ^{d,f}	1.2×10^5	1.8×10^5	8.6×10^4
18 PMC	78.2 ^c 79.3 ^d	2.5×10^8	3.4×10^8	1.7×10^8

^aError $\pm 5\%$. ^bFrom ref 14. ^cExperimental values in benzene from ref 25. ^dCalculated values in benzene from ref 26. ^eThe BDE value for the weaker O–H bond in the 4-position. ^fBDE value for the 3'-O–H catecholic bond in the isomer (–)-epicatechin.

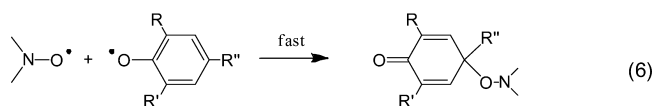
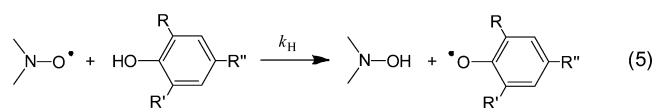
solution containing 1 M dicumyl peroxide (eq 2).^{20,21} The hydrogen transfer from the *N*-hydroxy derivatives to the cumyloxy radical occurs in competition with β -scission of the latter, which leads to the formation of acetophenone and a methyl radical (eq 4, $k_\beta \approx 6.5 \times 10^5 s^{-1}$ in CH₃CN²⁰).

After 355 nm laser excitation of a solution of dicumyl peroxide (1 M) and *N*-OH derivatives (5 mM) in N₂ saturated CH₃CN at 25 °C, the time-resolved spectra showed that the cumyloxy radical, characterized by an absorption centered at 485 nm,²¹ undergoes a first-order decay accompanied by a buildup of the absorption of the *N*-oxyl radicals. Absorption spectra of *N*-oxyl radicals 4-CO₂CH₃-PINO and 4-OCH₃-PINO are reported in the Supporting Information, Figures S1–S2, while those of PINO, 6-*Y*-BTNOs, QONO, and BONO have been reported in previous studies.^{2,22,23} The values of the visible absorption maximum wavelengths (λ_{max}) are given in Tables 1–3.

The *N*-oxyl radicals 1–8 are stable on the millisecond time scale. When an excess of phenolic compound (0.05–5 mM) is added, a fast first-order decay of radicals 1–8 was observed. As found in the LFP experiments of the hydrogen atom transfer promoted by PINO,¹⁴ with the exception of 2,2,5,7,8-pentamethylchroman-6-ol (PMC), no transient signals that could be assigned to phenoxyl radicals at ca. 380–400 nm were observed.²⁴ Thus, the k_H value for the hydrogen transfer from the phenolic O–H group of compounds 9–18 to the *N*-oxyl radicals 1–8 (eq 5 in Scheme 3) is significantly lower than the rate of combination of the phenoxyl radicals with the *N*-oxyl radicals (eq 6 in Scheme 3).

When the pseudo-first-order rate constants (k_{obs}) for the decay of the *N*-oxyl radicals measured at the maximum absorption wavelengths (see Table 1) were plotted against the concentration

Scheme 3



of phenolic compounds, excellent linear dependencies were observed. As an example, Figure 1 shows the plots of k_{obs} for the decay of the BTNO radical measured at 480 nm versus the concentration of 4-*Z*-2,6-(CH₃)₂C₆H₂OH (Z = OCH₃, NHCOCH₃, CH₃, H, Br) in CH₃CN at $T = 25$ °C. The k_{obs} vs [substrate] plots for the reactions of the *N*-oxyl radicals 1–8 with phenols 9–18 are reported in the Supporting Information as Figures S3–S16.

The second-order rate constants for the hydrogen transfer from the phenolic O–H to *N*-oxyl radicals (k_H) were obtained from the slopes of these plots using eq 7 for the reactions with phenols 9–17 ($k_{obs} = k_H[\text{PMC}]$ for the reaction of 2–8 with PMC). The k_H values are reported in Table 1 for the reactions promoted by 4-*X*-PINO, in Table 2 for the reactions with 6-*Y*-BTNOs, and in Table 3 for the reactions with QONO and BONO.

$$k_{obs} = 2k_H[\text{ArOH}] \quad (7)$$

Theoretical Calculations. Bond Dissociation Enthalpies. The computed O–H bond dissociation enthalpies (BDE_{NO-H})

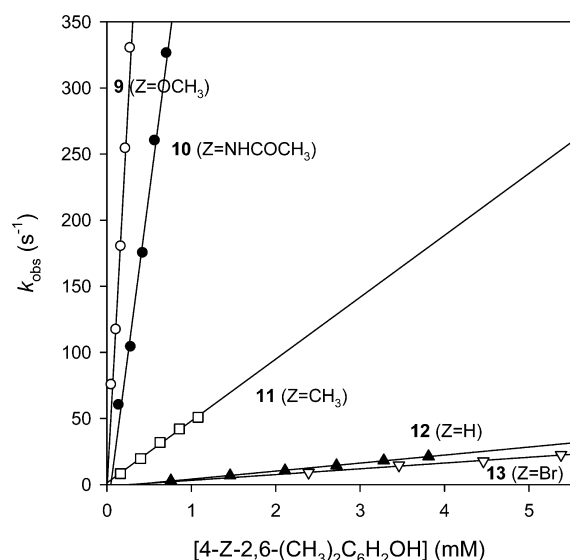


Figure 1. Dependence of k_{obs} for the decay of the BTNO radical measured at 480 nm on the concentration of 4-Z-2,6-(CH₃)₂C₆H₂OH (Z = OCH₃, NHCOCH₃, CH₃, H, Br) in CH₃CN at $T = 25$ °C.

for the *N*-hydroxylamines **1H**–**8H** precursors of aminoxyl radicals **1**–**8** were calculated by using the composite CBS-QB3 approach²⁷ as implemented in the Gaussian-09 program package.²⁸ The CBS-QB3 approach is capable of providing BDE values in agreement with experimental values to within about 1 kcal/mol.

The calculated BDE_{NO-H} values for **1H**–**8H** are reported in Table 4 along with available experimental values. BDEs for 4-*X*-NHPIs and 6-*Y*-HBTs were measured by the EPR or UV–vis radical equilibration technique.^{4,6,29} NHQO (**7H**) and NHBO

(**8H**) have calculated O–H BDEs that are larger than those of 4-*X*-NHPIs and 6-*Y*-HBTs, presumably owing to the differential stability of the resulting radicals. That is, radicals QONO and BONO contain 6-center, 7-electron rings, whereas 4-*X*-PINOs and 6-*Y*-BTNOs contain 5-center, 6-electron rings.

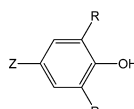
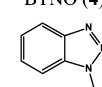
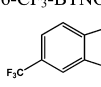
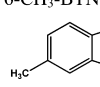
The computed gas-phase BDEs for 4-*X*-NHPIs and 6-*Y*-HBTs are significantly lower than the experimental BDE values measured in the polar solvents *t*BuOH and DMSO for NHPIs^{2c,6} and in acetonitrile for HBTs.²⁹ This finding is consistent with the previous computational work^{30–32} and may be attributed to the formation of hydrogen bonds with these solvents. For example, it was found that CH₃CN solvent can act as a hydrogen bond acceptor (HBA) forming a strong H-bond (ca. 7 kcal/mol) with NHPI, but none with PINO. Thus, the NO–H BDE of NHPI is enhanced by ca. 7 kcal/mol in such H-bonding solvent.³¹ The experimental BDE values for NHPI are also 5–7 kcal/mol higher than those calculated previously in the same solvents.³⁰ It was suggested that explicit solvent effects, where discrete solvent molecules are bound to the solute molecule, are required in order to adequately model the NO–H bond energy.

Ultimately, confidence in the calculated BDEs for **1H**–**8H** may, to some extent be derived from excellent correlation with the measured rate constants for the reactions with 2,6-dimethyl-4-methoxyphenol (vide infra).

Hydrogen Transfer Reactions. Density-functional theory (DFT) calculations were performed to model the reactions between *N*-oxyl radicals **1**–**8** and 4-methoxy-2,6-dimethylphenol (**9**) in order to analyze the structural effects of the *N*-oxyl radicals on the hydrogen transfer from an activated phenolic compound.

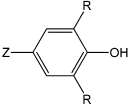
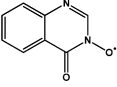
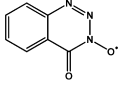
The B3LYP/6-31+G(2d,2p)^{34–37} approach was used. The effects of noncovalent interactions in the reacting systems were modeled with the dispersion-correcting potentials (DCPs) recently described.³⁸ Since DCPs have not yet been developed for the F atom, DCPs were applied to the H, C, N, and O atoms

Table 2. Second-Order Rate Constants k_{H} (M⁻¹ s⁻¹) for the Reaction of 6-Substituted Benzotriazole-*N*-oxyl Radicals (6-*Y*-BTNO, 4–6) with Phenols 9–18 Measured at $T = 25$ °C

	k_{H} (M ⁻¹ s ⁻¹) ^a		
	BTNO (4)  $\lambda_{\text{max}}=480$ nm	6-CF ₃ -BTNO (5)  $\lambda_{\text{max}}=450$ nm	6-CH ₃ -BTNO (6)  $\lambda_{\text{max}}=480$ nm
9 R=CH ₃ , Z=OCH ₃	1.3×10^6	6.5×10^6	1.2×10^6
10 R=CH ₃ , Z=NHCOCH ₃	4.9×10^5	2.0×10^6	3.9×10^5
11 R=CH ₃ , Z=CH ₃	4.5×10^4	1.6×10^5	4.3×10^4
12 R=CH ₃ , Z=H	6.2×10^3	1.4×10^4	6.0×10^3
13 R=CH ₃ , Z=Br	4.4×10^3	9.3×10^3	4.3×10^3
14 R= <i>t</i> Bu, Z=OCH ₃	2.2×10^5	7.0×10^5	2.0×10^5
15 R= <i>t</i> Bu, Z=CH ₃	1.4×10^4	2.7×10^4	1.3×10^4
16 Caffeic acid	3.4×10^4	8.2×10^4	3.1×10^4
17 (+)-Catechin	5.4×10^4	1.4×10^5	4.3×10^4
18 PMC	7.0×10^7	3.6×10^8	6.0×10^7

^aError ±5%.

Table 3. Second-Order Rate Constants k_H ($M^{-1} s^{-1}$) for the Reaction of 3-Quinazolin-4-one-*N*-oxyl Radical (QONO, 7) and 3-Benzotriazin-4-one-*N*-oxyl Radical (BONO, 8) with Phenols 9–18 Measured at $T = 25$ °C

	k_H ($M^{-1} s^{-1}$) ^a	
	QONO (7)  $\lambda_{max}=480$ nm	BONO (8)  $\lambda_{max}=450$ nm
9 R=CH ₃ , Z=OCH ₃	1.5×10^7	1.4×10^7
10 R=CH ₃ , Z=NHCOCH ₃	4.5×10^6	4.9×10^6
11 R= CH ₃ , Z=CH ₃	8.8×10^5	7.2×10^5
12 R= CH ₃ , Z=H	1.4×10^5	7.4×10^4
13 R= CH ₃ , Z=Br	8.4×10^4	4.5×10^4
14 R= <i>t</i> Bu, Z=OCH ₃	1.0×10^6	9.4×10^5
15 R= <i>t</i> Bu, Z=CH ₃	1.1×10^5	5.8×10^4
16 Caffeic acid	6.4×10^5	3.0×10^5
17 (+)-Catechin	6.6×10^5	4.3×10^5
18 PMC	3.4×10^8	6.1×10^8

^aError $\pm 5\%$.

Table 4. Calculated and Experimental BDE_{NO-H} Values for *N*-Hydroxylamines 1H–8H Precursors of *N*-Oxyl Radicals 1–8

	BDE _{NO-H} ^a		exptl
	calculated CBS-QB3		
	BDE	Δ BDE ^b	
NHPI (1H)	83.2 ^{c,d,e}	-4.4	87.0 ^f 89.6 ^g
4-CO ₂ CH ₃ -NHPI (2H)	83.4	-4.6	87.8 ^{f,h}
4-CH ₃ O-NHPI (3H)	83.0 ⁱ	-4.2	86.2 ^{f,h}
HBT (4H)	78.0	+0.8	85.1 ^j
6-CF ₃ -HBT (5H)	78.6	+0.2	86.5 ^j
6-CH ₃ -HBT (6H)	77.1	+1.7	85.3 ^j
NHQO (7H)	89.0	-10.2	nd
NHBO (8H)	89.1	-10.3	nd

^a In kcal/mol. ^b Computed as the difference between 2,6-dimethyl-4-methoxyphenol (9), for which the CBS-QB3 calculated O–H BDE is 78.8 kcal/mol, and 1H to 8H. ^c Calculated as 83.0 kcal/mol with the G3B3 method in vacuum, and 83.6 kcal/mol in acetonitrile; see ref 30. ^d Calculated as 81.2 kcal/mol using a correction of the result of a DFT method to approach G2M computed BDE; see ref 31. ^e Calculated as 80.8 kcal/mol using B3LYP/6-311+G*, see ref 32. ^f In *t*BuOH, from ref 6; the value was re-evaluated to be lower by 1.1 kcal/mol on the basis of the recalculated phenolic O–H BDE of the reference compound 4-methyl-2,6-di-*tert*-butylphenol (BHT) (ref 33). ^g Calculated by a thermochemical cycle in DMSO, from ref 2c. ^h From ref 4. ⁱ Calculated as 79.9 kcal/mol using B3LYP/6-311+G*; see ref 32. ^j From ref 29.

in systems containing 6-CF₃-BTNO. It has been demonstrated that DCPs offer incremental improvements to the description of noncovalent interactions as they are applied to each atom type in a system.³⁹

A single imaginary vibration mode connecting a π -stacked pre-reaction complex to a π -stacked post-reaction complex verified

activated complex structures. It has previously been shown that the reaction between PINO and 2,6-dimethyl-4-methoxyphenol occurs along a path through a stacked, “cisoid” complex and that the reaction through a nonstacked, “transoid” activated complex is much higher in energy.¹⁴

Estimations of the effects of acetonitrile solvent were obtained at the B3LYP-DCP/6-31+G(2d,2p) level of theory using a SMD continuum solvent model⁴⁰ applied to the gas-phase optimized structures. Figure 2a and b show the gas-phase optimized cisoid

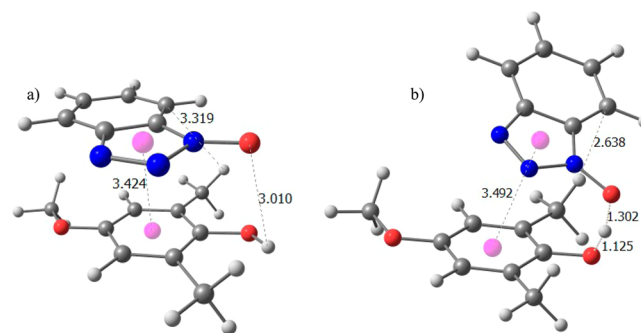


Figure 2. (a) Cisoid (π -stacked) pre-reaction complex formed by BTNO and 4-methoxy-2,6-dimethylphenol (9). (b) Cisoid transition state structure for the hydrogen transfer process. Ring centers are indicated by the light purple spheres. Some key distances are shown in angstroms.

pre-reaction and activated complexes for BTNO + 2,6-dimethyl-4-methoxyphenol (9). The structures shown in Figure 2 are quite representative of those associated with the pre-reaction and TS structures for the reaction of all of the *N*-oxyl radicals with the phenol. The coordinates for these complexes are reported in the Supporting Information. As described above, the stacked structure that is adopted in the activated complex allows for

Table 5. Calculated Gas-Phase Binding Energies (ΔE), Gas-Phase/Acetonitrile Solvent-Phase Free Energies, Relative to Reactants, of the Pre-reaction Complex (ΔG) and Transition State (TS) Complex (ΔG^\ddagger), Free Energy Variation ($\Delta BDFE$) for the Reactions of *N*-Oxyl Radicals 1–8 with 4-Methoxy-2,6-dimethylphenol (9) as Obtained from B3LYP-DCP/6-31+G(2d,2p) Calculations, Calculated Solvent-Phase Rate Constants ($k_{\text{H calc}}$), Experimental Rate Constants Measured in Acetonitrile ($k_{\text{H expt}}$), and Net Positive Charge on the Phenoxy Moiety at the TS (q_{ArO}^\ddagger)

reaction	ΔE^a	ΔG^a	ΔG^\ddagger^a	$\Delta BDFE^a$	$10^{-6} k_{\text{H calc}}^b$	$10^{-6} k_{\text{H expt}}^b$	q_{ArO}^\ddagger
9 + PINO (1)	-13.3	-0.2/4.4	4.1/7.7	-4.2	15.1	5.4	0.17
9 + 4-CO ₂ CH ₃ -PINO (2)	-14.6	-1.1/3.5	2.7/6.9	-6.0	57.3	4.2	0.20
9 + 4-CH ₃ O-PINO (3)	-13.4	0.4/4.7	4.1/7.8	-4.1	8.9	8.9	0.15
9 + BTNO (4)	-9.9	2.4/5.1	6.8/8.2	3.8	5.7	1.3	0.08
9 + 6-CF ₃ -BTNO (5)	-11.8	1.3/4.6	5.1/6.6	-0.1	88.3	1.2	0.12
9 + 6-CH ₃ -BTNO (6)	-10.3	1.8/4.6	7.0/8.5	4.3	3.8	6.5	0.07
9 + QONO (7)	-12.7	0.6/5.6	3.3/7.1	-10.7	38.5	15	0.12
9 + BONO (8)	-12.5	0.7/4.5	3.9/5.8	-11.0	330.6	14	0.15

^a In kcal/mol. ^b In M⁻¹ s⁻¹

the orbitals of the nitroxyl and phenol ring moieties to overlap as the hydrogen atom is transferred between them.

The free energies associated with the pre-reaction and TS structures, along with the calculated rate constants for the reactions of the *N*-oxyl radicals 1–8 with 4-methoxy-2,6-dimethylphenol, relative to the separated reactants, are listed in Table 5. The binding energies, defined as the negative of the electronic energy difference between the complex and its infinitely separated constituents, are also provided in Table 5.

The gas-phase binding energies associated with the pre-reaction complexes are quite large, ranging from 9.9 to 14.6 kcal/mol depending on the *N*-oxyl radical.⁴¹ The gas-phase binding free energies are considerably smaller in magnitude, with all of the complexes except PINO·9 and 4-CO₂CH₃-PINO·9 predicted to be unbound relative to the separated monomers. This is consistent with the loss in entropy associated with the formation of a dimer from two monomers. The inclusion of solvent effects via a continuum model simulating acetonitrile makes all of the binding free energies positive. This indicates that the solvent model predicts the preferential solvation of the monomers over the complexes. Overall, the calculations predict equilibrium constants for complexation of the *N*-oxyl radicals with 4-methoxy-2,6-dimethylphenol in the range of 2.7×10^{-3} to $7.8 \times 10^{-5} \text{ M}^{-1}$.⁴²

The calculated gas- and solvent-phase free energies of the TS complexes relative to separated reactants are also presented in Table 5. These data show that gas-phase reaction free-energy barriers are between 1.5 and 4.2 kcal/mol lower than the corresponding solvent-phase values. Bearing in mind that a 1.3 kcal/mol difference in barrier height corresponds to a 1 order of magnitude change in rate constant, the differences in gas- and solvent-phase barrier heights are significant. Using the solvent-phase free-energy barriers to compute the rate constants for the reactions produces fair to good results, with $k_{\text{calc}}/k_{\text{expt}}$ ranging from 2 to 24. This agreement between calculated and experimental rate constants lends support to a reaction mechanism involving a stacked activated complex structure.

DISCUSSION

As reported previously for the hydrogen transfer reactions promoted by PINO,¹⁴ a significant variation of the rate constants is observed by changing the phenolic structure with all the *N*-oxyl radicals investigated. The most reactive phenol, 2,2,5,7,8-pentamethylchroman-6-ol (PMC), is ca. 4 orders of magnitude more reactive than the least reactive, 4-bromo-2,6-dimethylphenol.

In the series of the *ortho*-dimethylated phenols 9–13 and *tert*-butylated phenols 14 and 15, rate constants increase with the electron-donating ability of the substituent, reflecting both enthalpic and polar effects. Electron-donating groups reduce the bond dissociation enthalpy (BDE) of the phenolic O–H bond (see Table 1) as a result of the stabilization of the phenoxy radical and destabilization of the phenol.^{33,43,44} As for the polar effects, it has to be considered that the reaction occurs by a HAT mechanism with a contribution from charge transfer occurring between the π -stacked phenolic and *N*-oxyl aromatic rings in a cisoid activated complex, as indicated by the calculations (see Figure 2 for the reaction of BTNO with 4-methoxy-2,6-dimethylphenol). Thus, an increase of the electron-donating properties of the phenolic substituents leads to an increased stabilization of the partial positive charge that develops on the phenolic ring in the activated complex. In accordance with a charge separation in the activated complex of the hydrogen transfer process, high and negative ρ values (Table 6) ranging

Table 6. ρ Values Calculated from the Hammett Correlation in the Reactions of *N*-Oxyl Radicals 1–8 with 4-*X*-2,6-Dimethylphenols (9–13) in CH₃CN at 25°C

<i>N</i> -oxyl radical	ρ^b
PINO (1) ^a	-2.76 (0.993)
4-CO ₂ CH ₃ -PINO (2)	-2.93 (0.976)
4-CH ₃ O-PINO (3)	-2.85 (0.982)
BTNO (4)	-2.85 (0.987)
6-CF ₃ -BTNO (5)	-3.21 (0.991)
6-CH ₃ -BTNO (6)	-2.74 (0.988)
QONO (7)	-2.45 (0.996)
BONO (8)	-2.78 (0.995)

^aFrom ref 14. ^b r^2 values are reported in parentheses.

from the least selective QONO ($\rho = -2.45$) to the most selective 6-CF₃BTNO ($\rho = -3.21$) were determined when the $\log(k_{\text{H}}^{\text{X}}/k_{\text{H}}^{\text{H}})$ values for the reactions of *N*-oxyl radicals 1–8 with phenols 9–13 were plotted versus the substituent constants σ^\ddagger .

As an example, Figure 3 shows a Hammett plot for the reactions of 4-*Z*-2,6-(CH₃)₂C₆H₂OH with BTNO. The Hammett plots for the reactions promoted by *N*-oxyl radicals 2, 3, and 5–8 are reported in Figures S17–S22 in the Supporting Information.

In all cases the ρ values are significantly more negative than that found in the hydrogen transfer reaction from 4-substituted-2,6-dimethylphenols to the styrylperoxy radical ($\rho = -1.36$),⁴⁵

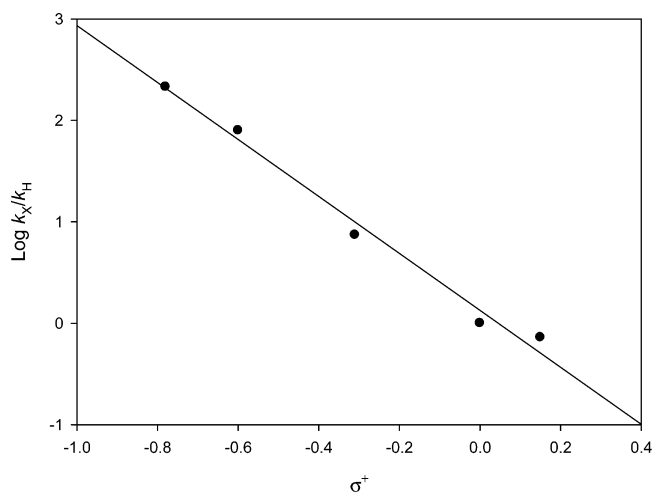


Figure 3. Hammett plot for the reactions of 4-Z-2,6-(CH₃)₂C₆H₂OH (9–13) with BTNO (4) in CH₃CN at 25 °C.

in accordance with the greater development of electron deficiency in the phenolic ring in the activated complex for HAT promoted by the *N*-oxyl radicals with respect to the peroxy radical (vide infra).

The importance of polar effects can be also evinced from the analysis of the reactivity data for the hydrogen transfer from the natural catecholic antioxidants (caffeic acid **16** and (+)-catechin **17**) and the simplified model of α -tocopherol, 2,2,5,7,8-pentamethylchroman-6-ol (PMC, **18**). The rate constants for the three phenolic compounds are in the order $k_H(\mathbf{18}) > k_H(\mathbf{17}) > k_H(\mathbf{16})$, as expected on the basis of the calculated BDE values²⁶ reported in Table 1. However, with PMC, k_H values are ca. 3 orders of magnitude higher than those observed with the two catecholic substrates, a difference that cannot be rationalized on enthalpic grounds in view of the small difference in the BDE values (less than 2 kcal/mol). The remarkable difference in reactivity between PMC and caffeic acid or (+)-catechin can be reasonably explained with the operation of polar effects. Accordingly, for PMC a greater stabilization of the partial positive charge that develops in the activated complex of the HAT process has to be expected in view of the much lower adiabatic ionization potentials (IP) for PMC calculated in benzene with respect to caffeic acid or (+)-catechin (136, 152, and 159 kcal/mol for PMC, (+)-catechin, and caffeic acid, respectively).²⁶

The k_H values are significantly influenced by steric effects of the phenolic *ortho*-substituents as previously observed in the reactions with the PINO radical.¹⁴ As such, the k_H values for 4-methoxy-2,6-dimethylphenol (**9**) and 2,4,6-trimethylphenol (**11**) are always much higher than those measured for 4-methoxy-2,6-di-*tert*-butylphenol (**14**) and 4-methyl-2,6-di-*tert*-butylphenol (**15**) even though the former reactions are 1.4–1.7 kcal mol⁻¹ less exothermic (see Table 1). Steric effects are also dependent on the structure of the *N*-oxyl radicals. Accordingly the decrease of reactivity observed by replacing the *ortho* dimethyl with the *ortho* di-*tert*-butyl substituents is lower with the less hindered 6-Y-BTNOs and higher with the 4-X-PINOs.

The analysis of the structural effects of the *N*-oxyl radical on hydrogen transfer reactions from the series of activated phenols represents the main objective of this study. From the kinetic data reported in Tables 1–3 it can be noted that significant variations of k_H are observed by changing the structure of the *N*-oxyl radical. For example in the reaction of the 4-methoxy-2,6-dimethylphe-

nol a 12-fold difference in k_H is observed between the least reactive 6-CH₃-BTNO ($k_H = 1.2 \times 10^6 \text{ M}^{-1} \text{ s}^{-1}$) and the most reactive QONO ($k_H = 1.5 \times 10^7 \text{ M}^{-1} \text{ s}^{-1}$). A fairly good linear correlation is obtained by plotting the experimental k_H values for the hydrogen transfer from 4-methoxy-2,6-dimethylphenol to the *N*-oxyl radicals **1–8** ($\ln k_{H \text{ expt}}$) and the free energy variation calculated for the same process in acetonitrile (ΔBDFE , see Table 5) (Figure 4).

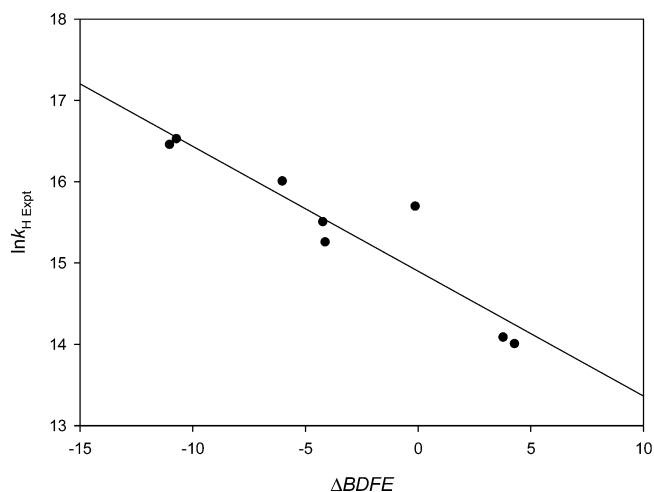


Figure 4. Correlation of experimental k_H values measured in acetonitrile ($\ln k_{H \text{ expt}}$) and the free energy variation calculated for the hydrogen transfer from 4-methoxy-2,6-dimethylphenol (**9**) to *N*-oxyl radicals **1–8** (ΔBDFE).

In the series of the substituted 4-X-PINOs (**1–3**) and 6-Y-BTNOs (**4–6**) it can be noted that substituents exert a significant effect on the rate constants for hydrogen transfer from all the phenolic substrates. The reactivity increases by increasing the electron-withdrawing properties of the aryl substituent as found in hydrogen abstraction processes from C–H bonds^{4,5,7d,8h,29,32,46} in accordance with the influence of both enthalpic and polar effects. From an enthalpic point of view, it has to be considered that BDE_{NO-H} values regularly increase with increasing electron-withdrawing (EW) power of the aryl substituents.^{4,29,32} The BDE_{NO-H} values calculated for **1H–8H** are reported in Table 4 together with the calculated values reported for NHPI and 4-OCH₃-NHPI^{30–32} and the experimental values determined for 4-X-NHPIs and 6-Y-HBTs by the EPR and UV–vis radical equilibration technique.^{4,6,29}

Substituent effects on the BDE_{NO-H} values have been explained on the basis of the destabilization provided by EW substituents to the charge-separated resonance structure of the *N*-oxyl radical as shown in Figure 5.^{4,29}

As described above the reactivity of *N*-oxyl radicals in the hydrogen atom transfer from activated phenols is determined not only by the enthalpic requirements of the ArO–H and NO–H

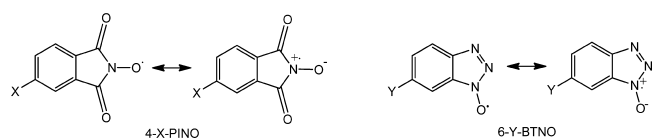


Figure 5. Resonance structures for 4-substituted phthalimide-*N*-oxyl radicals (4-X-PINO) and 6-substituted benzotriazole-*N*-oxyl radicals (6-Y-BTNO).

bond dissociation energies but also by the polar effects that may provide stabilization to the activated complex. Thus, the presence of electron-withdrawing substituents in the *N*-oxyl radicals confers additional stabilization to the activated complex and assists the development of the partial negative charge on the abstracting *N*-oxyl radical as mirrored by the favorable effect, described above, exerted by ED substituents on the phenolic nucleus where a partial positive charge develops (see Figure 6).

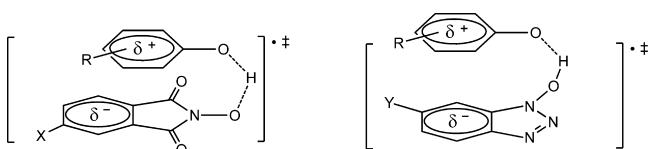


Figure 6. Cisoid (π -stacked) transition state structures for the hydrogen transfer from phenolic substrates promoted by 4-*X*-PINOs and 6-*Y*-BTNOs.

The results of theoretical calculations for the hydrogen transfer reactions between *N*-oxyl radicals 1–8 and 4-methoxy-2,6-dimethylphenol (9) permits an analysis of the structural effects of the *N*-oxyl radical on the charge transfer contribution to the activated complex. With all the *N*-oxyl radicals, the hydrogen transfer follows the same HAT mechanistic pathway described in the previous study on the reactions promoted by PINO.¹⁴ A cisoid-type pre-reaction complex is formed between the reactants (Figure 2) with stabilization energies that depend marginally on the structure of the *N*-oxyl radical (Table 5). The pre-reaction complexes formed by 4-*X*-PINO radicals are characterized by a higher degree of stabilization relative to separated reactants in the series of the *N*-oxyl radicals investigated with gas-phase binding energies (ΔE) ranging from -13.3 and -14.6 kcal/mol, while the 6-*Y*-BTNO radicals form the less stabilized complex ($-11.8 < \Delta E < -9.9$ kcal/mol).

From the pre-reaction complex, the reaction proceeds by a HAT process through a π -stacked cisoid activated complex in which the phenolic OH group is rotated so that it is pointing toward the singly occupied oxygen p-orbital of the *N*-oxyl radical (see Figure 2 for the reaction with BTNO). The π -stacking in the activated complex with the bonding π - π overlap involving the phenol and *N*-oxyl rings determines a significant degree of charge transfer (CT) from the phenolic ring to the *N*-oxyl ring, which is responsible for the remarkable polar effects observed in the hydrogen transfer process. To investigate the role of charge transfer in the hydrogen atom transfer reactions and its dependence on the structure of the *N*-oxyl radicals, the relationship between the rate constants for the hydrogen transfer process and the partial positive charge on the phenoxyl moiety of 9 in the activated complex ($q_{\text{ArO}}^{\ddagger}$ in Table 5) has been evaluated. In the series of aryl-substituted 4-*X*-PINOs and 6-*Y*-BTNOs, as expected, there is a regular increase in electron deficiency of the phenolic groups with increasing EW properties of the *N*-oxyl radical substituents. The relatively small positive charge that develops in the phenolic ring in the activated complex of the reactions with BONO and QONO can be attributed to the fact that the reactions are the most exergonic. Thus, the activated complex is more reactant-like, and the degree of charge transfer is less pronounced.

The important contribution of charge transfer in the reaction of *N*-oxyl radicals with activated phenols is highlighted by the comparison of the rate constants for reaction with 2,2,5,7,8-pentamethylchroman-6-ol (PMC) (Tables 1–3) with that

previously reported for HAT from α -tocopherol by the cumylperoxy radical ($3.8 \times 10^5 \text{ M}^{-1} \text{ s}^{-1}$ in CH_3CN).^{16,47} *N*-Oxyl radicals 1–8 are at least 2 orders of magnitude more reactive than CumOO^\bullet in hydrogen atom transfer from O–H bonds in activated phenols despite the similar bond dissociation energies of the O–H bonds in *N*-hydroxylamines and alkylhydroperoxides.^{15,48} Comparison of the k_{H} values determined in this study with those previously reported for hydrogen atom transfer to an alkylperoxy radical would suggest that the least reactive 6- CH_3 -BTNO may be the best candidate to be used as a model for evaluating the radical scavenging ability of phenolic antioxidants.

CONCLUSIONS

π -Stacking interactions between the phenolic and *N*-oxyl aromatic groups play an important role in the hydrogen atom transfer reactions from activated phenols, including the natural phenolic antioxidants caffeic acid and (+)-catechin, to short-lived *N*-oxyl radicals. The hydrogen transfer rate constants increase with the electron-donating strength of the phenolic ring substituent and with the electron-withdrawing (EW) power of the *N*-oxyl aryl substituent reflecting both enthalpic and polar effects. As for the enthalpic effects theoretical calculations show that electron-withdrawing groups increase the NO–H BDE in the *N*-hydroxylamine precursor of the *N*-oxyl radicals. For the polar effects, the analysis of the structural effects of the *N*-oxyl radicals on the role played by charge transfer interactions in the hydrogen transfer reactions from 4-methoxy-2,6-dimethylphenol showed a regular increase in the development of positive charge in the phenolic ring and a corresponding negative charge in the *N*-oxyl aryl ring by increasing the EW properties of the *N*-oxyl radical substituents.

The contribution from π -stacking interactions may be also relevant in the hydrogen atom transfer reactions from benzylic C–H bonds to short-lived *N*-oxyl radicals. Information in this respect will be provided by kinetic studies and theoretical calculations of hydrogen transfer reactions from alkylaromatics, benzylic alcohols, and benzylamines to short-lived *N*-oxyl radicals, which are currently being performed.

EXPERIMENTAL SECTION

Materials. CH_3CN (spectrophotometric grade), dicumyl peroxide, 1-hydroxybenzotriazole (HBT, 4H), 6-trifluoromethyl-1-hydroxybenzotriazole (6- CF_3 -HBT, 5H), and 6-hydroxybenzotriazin-4-one (NHBO, 8H) were used as received. 4-Methoxy-*N*-hydroxyphthalimide (4- OCH_3 -NHPI, 3H), 4-methoxycarbonyl-*N*-hydroxyphthalimide (4- CO_2CH_3 -NHPI, 2H), 6-methyl-1-hydroxybenzotriazole (6- CH_3 -HBT, 6H), and 3-hydroxy-quinazolin-4-one (NHQO, 7H) were synthesized according to the literature.^{4,22,23} Phenols 11–18 are commercially available and were further purified by sublimation. 4-Methoxy-2,6-dimethylphenol (9)⁴⁹ and *N*-(3,5-dimethyl-4-hydroxyphenyl)-acetamide (10) were synthesized using previously reported procedures.⁵⁰

Laser Flash Photolysis Experiments. Laser flash photolysis experiments were carried out with an Applied Photophysics LK-60 laser kinetic spectrometer providing 8 ns pulses, using the third harmonic (355 nm) of a Quantel Brilliant-B Q-switched Nd:YAG laser. The laser energy was adjusted to ≤ 10 mJ/pulse by the use of the appropriate filter. A 3.5-mL Suprasil quartz cell (10 mm \times 10 mm) was used for all experiments. N_2 -saturated CH_3CN solutions of dicumyl peroxide (1 M), *N*-hydroxylamines 1H–8H (5.0 mM), and phenol 9–18 (0.05–5 mM) were used. All experiments were carried out at $T = 25 \pm 0.5$ °C under magnetic stirring. Data were collected at individual wavelengths with an Agilent Infinium oscilloscope and analyzed with the kinetic package provided with the instrument. Rate constants were obtained by monitoring the change of absorbance at the maximum absorption

wavelengths of the *N*-oxyl radicals 2–8 by averaging 3–5 values. Each kinetic trace exhibited first-order behavior. Second-order rate constants were obtained from the slopes of plots of the observed rate constants k_{obs} vs substrate concentration.

■ ASSOCIATED CONTENT

■ Supporting Information

Absorption spectra of 4-CO₂CH₃-PINO and 4-CH₃O-PINO. Dependence of k_{obs} for the decay of the *N*-oxyl radicals 1–8 on the concentrations of phenols 9–18. Hammett plots for the reactions of 4-*X*-2,6-(CH₃)₂C₆H₂OH with *N*-oxyl radicals 2, 3, 5–8. Optimized Cartesian coordinates of structures associated with the reactions of *N*-oxyl radicals 1–8 with 4-methoxy-2,6-dimethylphenol (9). This material is available free of charge via the Internet at <http://pubs.acs.org>.

■ AUTHOR INFORMATION

Corresponding Authors

*E-mail: Gino.DiLabio@ubc.ca.

*E-mail: osvaldo.lanzalunga@uniroma1.it.

Notes

The authors declare no competing financial interest.

■ ACKNOWLEDGMENTS

Thanks are due to the Ministero dell'Istruzione, dell'Università e della Ricerca (MIUR) for financial support, PRIN 2010-2011 (2010PFLRJR) project (PROxi project), and Westgrid for access to computational resources. We thank Prof. Lorenzo Stella for the use of LFP equipment.

■ REFERENCES

- (1) (a) Recupero, F.; Punta, C. *Chem. Rev.* **2007**, *107*, 3800–3842. (b) Coseri, S. *Catal. Rev.* **2009**, *51*, 218–292. (c) Tebben, L.; Studer, A. *Angew. Chem., Int. Ed.* **2011**, *50*, 5034–5068. (d) Wertz, S.; Studer, A. *Green Chem.* **2013**, *15*, 3116–3134. (e) Melone, L.; Punta, C. *Beilstein J. Org. Chem.* **2013**, *9*, 1296–1310.
- (2) (a) Ueda, C.; Noyama, M.; Ohmori, H.; Masui, M. *Chem. Pharm. Bull.* **1987**, *35*, 1372–1377. (b) Minisci, F.; Punta, C.; Recupero, F.; Fontana, F.; Pedulli, G. F. *J. Org. Chem.* **2002**, *67*, 2671–2676. (c) Koshino, N.; Cai, Y.; Espenson, J. H. *J. Phys. Chem. A* **2003**, *107*, 4262–4267. (d) Hermans, I.; Vereecken, L.; Jacobs, P. A.; Peeters, J. *Chem. Commun.* **2004**, 1140–1141. (e) Brandi, P.; Galli, C.; Gentili, P. *J. Org. Chem.* **2005**, *70*, 9521–9528. (f) Galli, C.; Gentili, P.; Lanzalunga, O. *Angew. Chem., Int. Ed.* **2008**, *47*, 4790–4796. (g) Chen, K.; Sun, Y.; Wang, C.; Yao, Y.; Chen, Z.; Li, H. *Phys. Chem. Chem. Phys.* **2012**, *14*, 12141–12146.
- (3) Minisci, F.; Recupero, F.; Cecchetto, A.; Gambarotti, C.; Punta, C.; Faletti, R.; Paganelli, R.; Pedulli, G. F. *Eur. J. Org. Chem.* **2004**, 109–119.
- (4) Annunziatini, C.; Gerini, M. F.; Lanzalunga, O.; Lucarini, M. *J. Org. Chem.* **2004**, *69*, 3431–3438.
- (5) Cai, Y.; Koshino, N.; Saha, B.; Espenson, J. H. *J. Org. Chem.* **2005**, *70*, 238–243.
- (6) Amorati, R.; Lucarini, M.; Mugnaini, V.; Pedulli, G. F.; Minisci, F.; Recupero, F.; Fontana, F.; Astolfi, P.; Greci, L. *J. Org. Chem.* **2003**, *68*, 1747–1754.
- (7) (a) Ishii, Y.; Nakayama, K.; Takeno, M.; Sakaguchi, S.; Iwahama, T.; Nishiyama, Y. *J. Org. Chem.* **1995**, *60*, 3934–3935. (b) Ishii, Y.; Iwahama, T.; Sakaguchi, S.; Nakayama, K.; Nishiyama, Y. *J. Org. Chem.* **1996**, *61*, 4520–4526. (c) Wentzel, B. B.; Donners, M. P. J.; Alsters, P. L.; Feiters, M. C.; Nolte, R. J. M. *Tetrahedron* **2000**, *56*, 7797–7803. (d) Ishii, Y.; Sakaguchi, S.; Iwahama, T. *Adv. Synth. Catal.* **2001**, *343*, 393–427. (e) Minisci, F.; Recupero, F.; Cecchetto, A.; Gambarotti, C.; Punta, C.; Paganelli, R. *Org. Proc. Res. Dev.* **2004**, *8*, 163–168. (f) Sheldon, R. A.; Arends, I. W. C. E. *Adv. Synth. Catal.* **2004**, *346*, 1051–1071. (g) Yang, G.; Ma, Y.; Xu, J. *J. Am. Chem. Soc.* **2004**, *126*, 10542–10543. (h) Yang, G.; Zhang, Q.; Miao, H.; Tong, X.; Xu, J. *Org. Lett.* **2005**, *7*, 263–266. (i) Ishii, Y.; Sakaguchi, S. *Catal. Today* **2006**, *117*, 105–113. (j) Sheldon, R. A.; Arends, I. W. C. E. *J. Mol. Catal. A* **2006**, *251*, 200–214. (k) Nechab, M.; Kumar, D. N.; Philouze, C.; Einhorn, C.; Einhorn, J. *Angew. Chem., Int. Ed.* **2007**, *46*, 3080–3083. (l) Lee, J. M.; Park, E. J.; Cho, S. H.; Chang, S. *J. Am. Chem. Soc.* **2008**, *130*, 7824–7825. (m) Zheng, G.; Liu, C.; Wang, Q.; Wang, M.; Yang, G. *Adv. Synth. Catal.* **2009**, *351*, 2638–2642. (n) Melone, L.; Gambarotti, C.; Prosperini, S.; Pastori, N.; Recupero, F.; Punta, C. *Adv. Synth. Catal.* **2011**, *353*, 147–154. (o) Aguadero, A.; Falcon, H.; Campos-Martin, J. M.; Al-Zahrani, S. M.; Fierro, J. L. G.; Alonso, J. A. *Angew. Chem., Int. Ed.* **2011**, *50*, 6557–6561. (p) Lin, R.; Chen, F.; Jiao, N. *Org. Lett.* **2012**, *14*, 4158–4161.

- (8) (a) Call, H. P.; Mücke, I. *J. Biotechnol.* **1997**, *53*, 163–202. (b) Sealey, B. J.; Ragauskas, A. J.; Elder, T. J. *Holzforchung* **1999**, *53*, 498–502. (c) Xu, F.; Kuly, J. J.; Duke, K.; Li, K.; Krikstopaitis, K.; Deussen, H.-J. W.; Abbate, E.; Galinyte, V.; Schneider, P. *Appl. Environ. Microbiol.* **2000**, *66*, 2052–2056. (d) Xu, F.; Deuss, H.-J. W.; Lopez, B.; Lam, L.; Li, K. *Eur. J. Biochem.* **2001**, *268*, 4169–4176. (e) D'Acunzo, F.; Baiocco, P.; Fabbrini, M.; Galli, C.; Gentili, P. *New J. Chem.* **2002**, *26*, 1791–1794. (f) Baiocco, P.; Barrea, A. M.; Fabbrini, M.; Galli, C.; Gentili, P. *Org. Biomol. Chem.* **2003**, *1*, 191–197. (g) Geng, X.; Li, K.; Xu, F. *Appl. Microbiol. Biotechnol.* **2004**, *64*, 493–496. (h) Annunziatini, C.; Baiocco, P.; Gerini, M. F.; Lanzalunga, O.; Sjögren, B. *J. Mol. Catal. B: Enzym.* **2005**, *32*, 89–96. (i) Branchi, B.; Galli, C.; Gentili, P. *Org. Biomol. Chem.* **2005**, *3*, 2604–2614. (j) Astolfi, P.; Brandi, P.; Galli, C.; Gentili, P.; Gerini, M. F.; Greci, L.; Lanzalunga, O. *New J. Chem.* **2005**, *29*, 1308–1317.
- (9) (a) Argyropoulos, D. S.; Menachem, S. B. *Biotechnology in the Pulp and Paper Industry*; Eriksson, K. E. L., Ed.; Springer-Verlag: Berlin Heidelberg, 1997; pp 127–158. (b) Moldes, D.; Cadena, E. M.; Vidal, T. *Bioresour. Technol.* **2010**, *101*, 6924–6929. (c) Valls, C.; Colom, J. F.; Baffert, C.; Gimbert, I.; Roncero, M. B.; Sigoillot, J.-C. *Biochem. Eng. J.* **2010**, *49*, 401–407. (d) Gutierrez, A.; Rencoret, J.; Cadena, E. M.; Rico, A.; Barth, D.; del Rio, J. C.; Martinez, A. T. *Bioresour. Technol.* **2012**, *119*, 114–122.
- (10) (a) Okazaki, S.; Michizoe, J.; Goto, M.; Furusaki, S.; Wariishi, H.; Tanaka, H. *Enzym. Microbiol. Technol.* **2002**, *31*, 227–232. (b) Gomez, S. J.; Rodriguez Solar, D.; Pazos, M.; Sanroman, M. A. *Biotechnol. Lett.* **2006**, *28*, 1013–1017. (c) Cambria, M. T.; Minniti, Z.; Librando, V.; Cambria, A. *Appl. Biochem. Biotechnol.* **2008**, *149*, 1–8. (d) Mizuno, H.; Hirai, H.; Kawai, S.; Nishida, T. *Biodegradation* **2009**, *20*, 533–539. (e) Hu, X.; Wang, P.; Hwang, H. *Bioresour. Technol.* **2009**, *100*, 4963–4968. (f) Torres-Duarte, C.; Roman, R.; Tinoco, R.; Vazquez-Duhalt, R. *Chemosphere* **2009**, *77*, 687–692. (g) Marco-Urrea, E.; Perez-Trujillo, M.; Blaquez, P.; Vicent, T.; Caminal, G. *Bioresour. Technol.* **2010**, *101*, 2159–2166. (h) Wong, K.-S.; Huang, Q.; Au, C.-H.; Wang, J.; Kwan, H.-S. *Bioresour. Technol.* **2012**, *104*, 157–164. (i) Suda, T.; Hata, T.; Kawai, S.; Okamura, H.; Nishida, T. *Bioresour. Technol.* **2012**, *103*, 498–501.
- (11) (a) Husain, Q. *Crit. Rev. Biotechnol.* **2006**, *26*, 201–221 and references therein. (b) Murugesan, K.; Nam, I.-H.; Kim, Y.-M.; Chang, Y.-S. *Enzym. Microbiol. Technol.* **2007**, *40*, 1662–1672. (c) Tavares, A. P. M.; Cristovao, R. O.; Gamelas, J. A. F.; Loureiro, J. M.; Boaventura, R. A. R.; Macedo, E. A. *J. Chem. Technol. Biotechnol.* **2009**, *84*, 442–446. (d) Chabra, M.; Mishra, S.; Sreekrishnan, T. R. *J. Biotechnol.* **2009**, *143*, 69–78. (e) Lu, L.; Zhao, M.; Li, G.-F.; Li, J.; Wang, T.-N.; Li, D.-B.; Xu, T.-F. *Catal. Commun.* **2012**, *26*, 58–62. (f) Chairin, T.; Nitheranont, T.; Watanabe, A.; Asada, Y.; Khanongnuch, C.; Lumyong, S. *Appl. Biochem. Biotechnol.* **2013**, *169*, 539–545.
- (12) (a) Potthast, A.; Rosenau, T.; Chen, C. L.; Gratzl, J. S. *J. Mol. Catal. A: Chem.* **1996**, *108*, 5–9. (b) Verkade, J. M. M.; van Hemert, L. J. C.; Quaedflieg, P. J. L. M.; Schoemaker, H. E.; Schuermann, M.; van Delft, F. L.; Rutjes, F. P. J. T. *Adv. Synth. Catal.* **2007**, *349*, 1332–1336. (c) Yang, Z.; Pattamana, K.; Molino, B. F.; Haydar, S. N.; Cao, Y.; Bois, F.; Maeng, J.-H.; Hemenway, M. S.; Rich, J. O.; Khmelitsky, Y. L.; Michels, P. C.; Friedrich, T. D.; Peace, D. *Synlett* **2009**, *18*, 2935–2938. (d) Bernini, R.; Crisante, F.; Gentili, P.; Morana, F.; Pierini, M.; Piras, M. *J. Org. Chem.* **2011**, *76*, 820–832.
- (13) Baciocchi, E.; Gerini, M. F.; Lanzalunga, O. *J. Org. Chem.* **2004**, *69*, 8863–8866.

- (14) D'Alfonso, C.; Bietti, M.; DiLabio, G.; Lanzalunga, O.; Salamone, M. *J. Org. Chem.* **2013**, *78*, 1026–1037.
- (15) Berkowitz, J.; Ellison, J. B.; Gutman, D. *J. Phys. Chem.* **1994**, *98*, 2744–2765.
- (16) Valgimigli, L.; Banks, J. T.; Luszyk, J.; Ingold, K. U. *J. Org. Chem.* **1999**, *64*, 3381–3383.
- (17) DiLabio, G. A.; Johnson, E. R. *J. Am. Chem. Soc.* **2007**, *129*, 6199–6203.
- (18) The previous kinetic investigation of the reactions of PINO with **9–15** and **18**¹⁴ has been now extended to the hydrogen abstraction process from the two catecholic substrates **16** and **17**.
- (19) (a) Baciocchi, E.; Bietti, M.; Di Fusco, M.; Lanzalunga, O. *J. Org. Chem.* **2007**, *72*, 8748–8754. (b) Baciocchi, E.; Bietti, M.; Gerini, M. F.; Lanzalunga, O. *J. Org. Chem.* **2005**, *70*, 5144–5149. (c) Coseri, S.; Mendenhall, G. D.; Ingold, K. U. *J. Org. Chem.* **2005**, *70*, 4629–4636.
- (20) Avila, D. V.; Brown, C. E.; Ingold, K. U.; Luszyk, J. *J. Am. Chem. Soc.* **1993**, *115*, 466–470.
- (21) (a) Avila, D. V.; Luszyk, J.; Ingold, K. U. *J. Am. Chem. Soc.* **1992**, *114*, 6576. (b) Avila, D. V.; Ingold, K. U.; Di Nardo, A. A.; Zerbetto, F.; Zgierki, M. Z.; Luszyk, J. *J. Am. Chem. Soc.* **1995**, *117*, 2711.
- (22) (a) Baciocchi, E.; Bietti, M.; Lanzalunga, O.; Lapi, A.; Raponi, D. *J. Org. Chem.* **2010**, *75*, 1378. (b) Baciocchi, E.; Bietti, M.; Di Fusco, M.; Lanzalunga, O.; Raponi, D. *J. Org. Chem.* **2009**, *74*, 5576–5583. (c) Galli, C.; Gentili, P.; Lanzalunga, O.; Lucarini, M.; Pedulli, G. F. *Chem. Commun.* **2004**, 2356.
- (23) Baciocchi, E.; Bietti, M.; D'Alfonso, C.; Lanzalunga, O.; Lapi, A.; Salamone, M. *Org. Biomol. Chem.* **2011**, *9*, 4085–4090.
- (24) (a) Das, P. K.; Encinas, M. V.; Steenken, S.; Scaiano, J. C. *J. Am. Chem. Soc.* **1981**, *103*, 4162–4166. (b) Shukla, D.; Schepp, N. P.; Mathivanan, N.; Johnston, L. J. *Can. J. Chem.* **1997**, *75*, 1820–1829.
- (25) Lucarini, M.; Pedrielli, P.; Pedulli, G. F.; Cabiddu, S.; Fattuoni, C. *J. Org. Chem.* **1996**, *61*, 9259–9263.
- (26) Leopoldini, M.; Marino, T.; Russo, N.; Toscano, M. *J. Phys. Chem. A* **2004**, *108*, 4916–4922.
- (27) Montgomery, J. A., Jr.; Frisch, M. J.; Ochterski, J. W.; Petersson, G. A. *J. Chem. Phys.* **2000**, *112*, 6532–6542.
- (28) Frisch, M. J.; Trucks, G. W.; Schlegel, H. B.; Scuseria, G. E.; Robb, M. A.; Cheeseman, J. R.; Scalmani, G.; Barone, V.; Mennucci, B.; Petersson, G. A.; Nakatsuji, H.; Caricato, M.; Li, X.; Hratchian, H. P.; Izmaylov, A. F.; Bloino, J.; Zheng, G.; Sonnenberg, J. L.; Hada, M.; Ehara, M.; Toyota, K.; Fukuda, R.; Hasegawa, J.; Ishida, M.; Nakajima, T.; Honda, Y.; Kitao, O.; Nakai, H.; Vreven, T.; Montgomery, J. A., Jr.; Peralta, J. E.; Ogliaro, F.; Bearpark, M.; Heyd, J. J.; Brothers, E.; Kudin, K. N.; Staroverov, V. N.; Kobayashi, R.; Normand, J.; Raghavachari, K.; Rendell, A.; Burant, J. C.; Iyengar, S. S.; Tomasi, J.; Cossi, M.; Rega, N.; Millam, N. J.; Klene, M.; Knox, J. E.; Cross, J. B.; Bakken, V.; Adamo, C.; Jaramillo, J.; Gomperts, R.; Stratmann, R. E.; Yazyev, O.; Austin, A. J.; Cammi, R.; Pomelli, C.; Ochterski, J. W.; Martin, R. L.; Morokuma, K.; Zakrzewski, V. G.; Voth, G. A.; Salvador, P.; Dannenberg, J. J.; Dapprich, S.; Daniels, A. D.; Farkas, Ö.; Foresman, J. B.; Ortiz, J. V.; Cioslowski, J.; Fox, D. J. *Gaussian 09*, Revision D.01; Gaussian, Inc.: Wallingford, CT, 2009.
- (29) D'Alfonso, C.; Lanzalunga, O.; Lapi, A.; Vadalà, R. *Tetrahedron* **2014**, *70*, 3049–3055.
- (30) Da Silva, G.; Bozzelli, J. W. *J. Phys. Chem. C* **2007**, *111*, 5760–5765.
- (31) Hermans, I.; Jacobs, P.; Peeters, J. *J. Phys. Chem. Chem. Phys.* **2007**, *9*, 686–690.
- (32) Sun, Y.; Zhang, W.; Hu, X.; Li, H. *J. Phys. Chem. B* **2010**, *114*, 4862–4869.
- (33) Mulder, P.; Korth, H.-G.; Pratt, D. A.; DiLabio, G. A.; Valgimigli, L.; Pedulli, G. F.; Ingold, K. U. *J. Phys. Chem. A* **2005**, *109*, 2647–2655.
- (34) Becke, A. D. *J. Chem. Phys.* **1993**, *98*, 5648–5652.
- (35) Lee, C.; Yang, W.; Parr, R. G. *Phys. Rev. B* **1988**, *37*, 785–789.
- (36) All calculations described herein were performed with the Gaussian-09 program package: Frisch, M. J.; Trucks, G. W.; Schlegel, H. B.; Scuseria, G. E.; Robb, M. A.; Cheeseman, J. R.; Scalmani, G.; Barone, V.; Mennucci, B.; Petersson, G. A. et al. *Gaussian 09*, revision C.01; Gaussian, Inc.: Wallingford, CT, 2009.
- (37) All molecule, radical, and pre-reaction complexes were verified to only positive vibration frequencies, whereas transition state structures for hydrogen atom transfer possessed a single imaginary vibration associated with the transfer of the H atom from 3-methoxy-2,6-dimethylphenol to the *N*-oxyl radicals **1–8**.
- (38) Torres, E.; DiLabio, G. A. *J. Phys. Chem. Lett.* **2012**, *3*, 1738–1744. For tools to generate input files incorporating DCPs, see also www.ualberta.ca/~gdilabio.
- (39) DiLabio, G. A.; Koleini, M. *J. Chem. Phys.* **2014**, *140*, No. 18A542.
- (40) Marenich, A. V.; Cramer, C. J.; Truhlar, D. G. *J. Phys. Chem. B* **2009**, *113*, 6378–6396.
- (41) For comparison, the gas-phase binding energy of the water dimer is about 5 kcal/mol. DiLabio, G. A.; Johnson, E. R.; Otero-de-la-Roza, A. *Phys. Chem. Chem. Phys.* **2013**, *15*, 12821–12828.
- (42) It occurred to us that the effects of solvent may result in open (viz., transoid) transition state complexes being favored over the stacked transition state complexes. Additional computations involving the PINO-9 supported the conclusions based on our original gas-phase calculations that the stacked transition state structure is favored over the transoid one by at least 5 kcal/mol in continuum acetonitrile solvent.
- (43) (a) Denisov, E. T.; Khudyakov, I. V. *Chem. Rev.* **1987**, *87*, 1313–1357. (b) Amorati, R.; Ferroni, F.; Pedulli, G. F.; Valgimigli, L. *J. Org. Chem.* **2003**, *68*, 9654–9658. (c) Johansson, H.; Shanks, D.; Engman, L.; Amorati, R.; Pedulli, G. F.; Valgimigli, L. *J. Org. Chem.* **2010**, *75*, 7535–7541. (d) Amorati, R.; Menichetti, S.; Mileo, E.; Pedulli, G. F.; Vigliani, C. *Chem.—Eur. J.* **2009**, *15*, 4402–4410.
- (44) (a) Wijtmans, M.; Pratt, D. A.; Valgimigli, L.; DiLabio, G. A.; Pedulli, G. F.; Porter, N. A. *Angew. Chem., Int. Ed.* **2003**, *42*, 4370–4373. (b) Pratt, D. A.; DiLabio, G. A.; Mulder, P.; Ingold, K. U. *Acc. Chem. Res.* **2004**, *37*, 334–340. (c) Wijtmans, M.; Pratt, D. A.; Brinkhorst, J.; Serwa, R.; Valgimigli, L.; Pedulli, G. F.; Porter, N. A. *J. Org. Chem.* **2004**, *69*, 9215–9223. (d) Shang, Y.-J.; Qian, Y.-P.; Liu, X.-D.; Dai, F.; Shang, X.-L.; Jia, W.-Q.; Liu, Q.; Fang, J.-G.; Zhou, B. *J. Org. Chem.* **2009**, *74*, 5025–5031.
- (45) Howard, J. A.; Ingold, K. U. *Can. J. Chem.* **1963**, *41*, 2800–2806.
- (46) Aweke Tadesse, M.; Galli, C.; Gentili, P. *J. Phys. Org. Chem.* **2011**, *24*, 529–538.
- (47) The latter process likely occurs by a mechanism involving PCET, wherein a proton is transferred between O atoms and an electron transferred via a peroxy oxygen lone pair-phenolic ring π overlap.¹⁷
- (48) Denisov, E. *Handbook of Antioxidants*; CRC Press: Boca Raton, 1995. Luo, Y.-R. *Comprehensive Handbook of Chemical Bond Energies*; CRC Press: Boca Raton, 2007.
- (49) Paterson, I.; Delgado, O.; Florence, G. J.; Lyothier, I.; O'Brien, M.; Scott, J. P.; Sereinig, N. *J. Org. Chem.* **2005**, *70*, 150–160.
- (50) Alisi, M. A.; Brufani, M.; Cazzolla, N.; Ceccacci, F.; Dragone, P.; Felici, M.; Furlotti, G.; Garofalo, B.; La Bella, A.; Lanzalunga, O.; Leonelli, F.; Marini Bettolo, R.; Maugeri, C.; Migneco, L. M.; Russo, V. *Tetrahedron* **2012**, *68*, 10180–10187.